The Advanced Virgo monolithic fused silica suspension

D. Aisa[2], S. Aisa[2], C. Campeggi[2], M. Colombini[2], A. Conte[3], L. Farnesini[2], E. Majorana[3], F. Mezzani[3], M. Montani[1], L. Naticchioni[3], M. Perciballi[3], F. Piergiovanni[1], A. Piluso[2], P. Puppo[3], P. Rapagnani[3], F. Travasso[2], A. Viceré[1], H. Vocca[2]

[1]University of Urbino and INFN Firenze
[2]University of Perugia and INFN Perugia
[3]University of Roma Sapienza and INFN Roma

Abstract

The detection of gravitational waves is one of the most challenging prospects faced by experimental physicists. Suspension thermal noise is an important noise source at operating frequencies between approximately 10 and 30 Hz, and represents a limit to the sensitivity of the ground based interferometric gravitational wave detectors. Its effects can be reduced by minimizing the losses and optimizing the geometry of the suspension fibre and its attachment system. In this poster we will present the design of last suspension system for use in the Advanced Virgo (AdV) detector, describing the design of the double stage monolithic suspension. With the help of a finite element model, we also present a full thermal noise analysis, taking into account for the precise geometry of the fibers attachment systems on the suspension elements. We shall demonstrate the suitability of this suspension for installation in AdV.

The mirror steering stage: the marionette

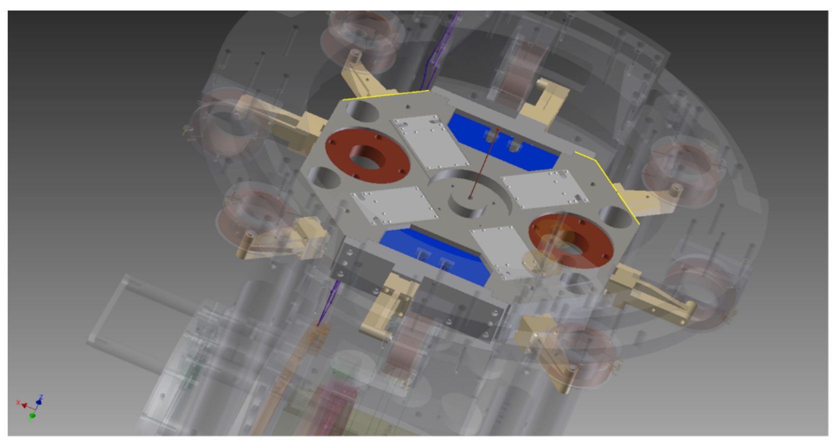

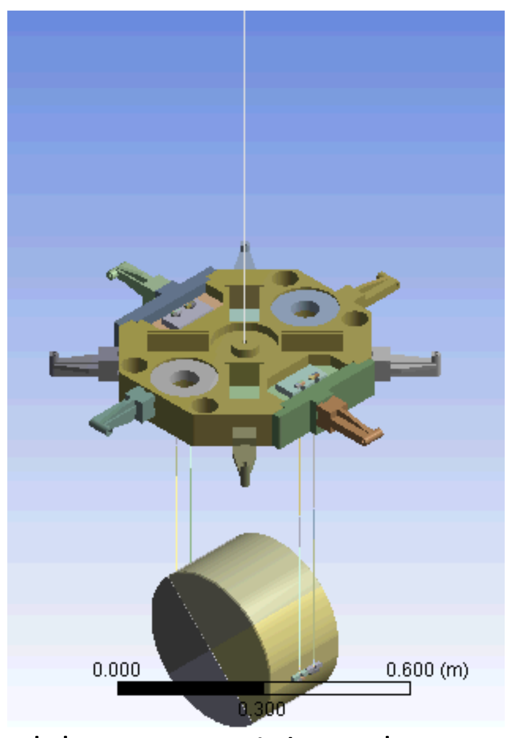

The *marionette* is the first stage of a simple double pendulum system. It is used to orientate the mirror in closed loop in order to keep its working position. The body of the marionette is made of amagnetic steel (AISI 216L). Eight dielectric supports (made of peek) are designed to hold the magnets of the electromagnetic actuators. The monolithic fiber clamping system, is shown in blue. The fibers are terminated by prism-shaped anchors. The upper ones are contacted to the marionette body through hydroxide-catalysis bonds (HCB), applied to a suitably polished, steel interface. The anchors at the bottom hold the mirror through suitable ears, contacted on the miser side flats by means of HCB.

Thermal Noise

Mode (ν) Hz	Q (10^6) (ITM,ETM)	Comments	Effective masses (kg) (ITM,ETM)
5735.00	107,52	Butterfly	
5741.00	59,37	Butterfly	
7842.00	107,50	Drum	25,28
9933	71,42	Butterfly	
9951	44,30	Butterfly	
10120	72,61	Longitudinal	76,78
13000	28,24	Longitudinal	18,19
14980	64,54	Longitudinal	9,11

We have developed a finite element model of the mirror and its suspension, including the coating, the upper and lower fiber clamps.
We have estimated the mirror modal losses: in the table above the expected Q for the Input and End mirrors modes and their effective masses are reported.
The suspension thermal noise including the contribution of the silicate bonding layers both at the marionette and the mirror level are shown in the plot on the left.

Silicate bonding layers geometrical and elastic properties used in the simulation.

Ears	
Layer Thickness	$60\ nm$
Bonded Area	$2\times 12.5\ cm^2$
Anchors	
Layer Thickness	$60\ nm$
Bonded Area	$4\times 1.6\ cm^2$
Magnets	
Layer Thickness	$60\ nm$
Bonded Area	$4\times$ *diameter* $6\ mm$
HCB	
Mechanical Properties	$\rho = 2200\ kg/m^3$ $Y = 7.9\ GPa$ $\sigma = 0.17$

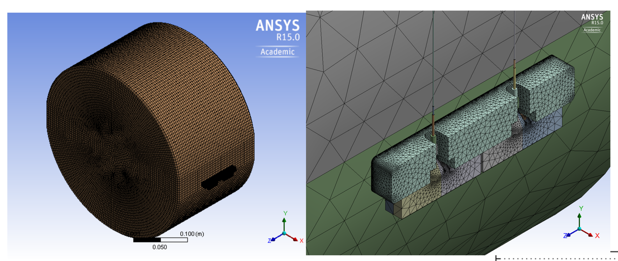

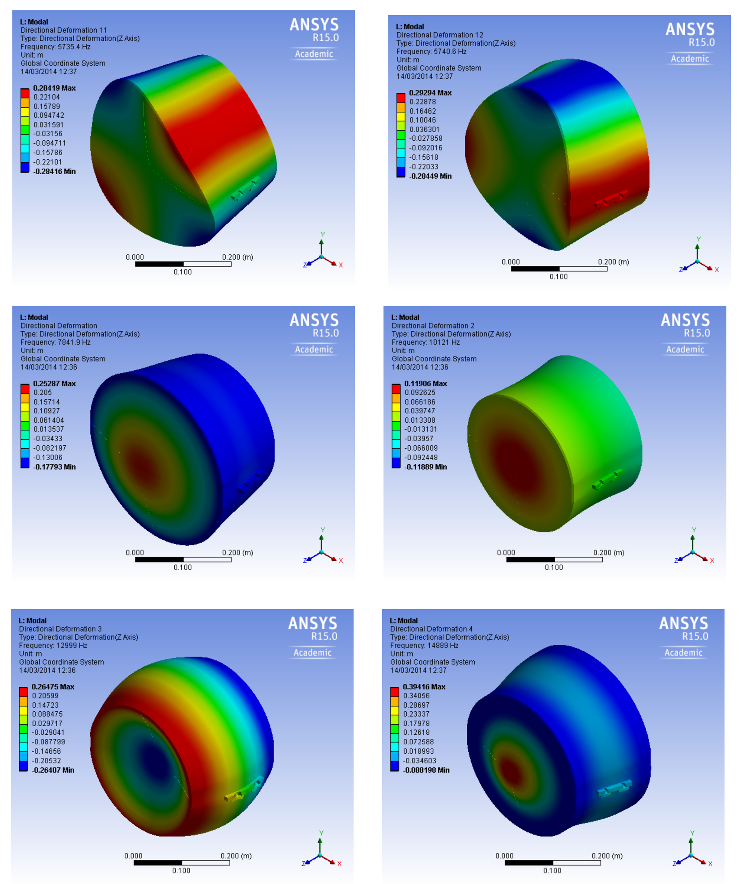

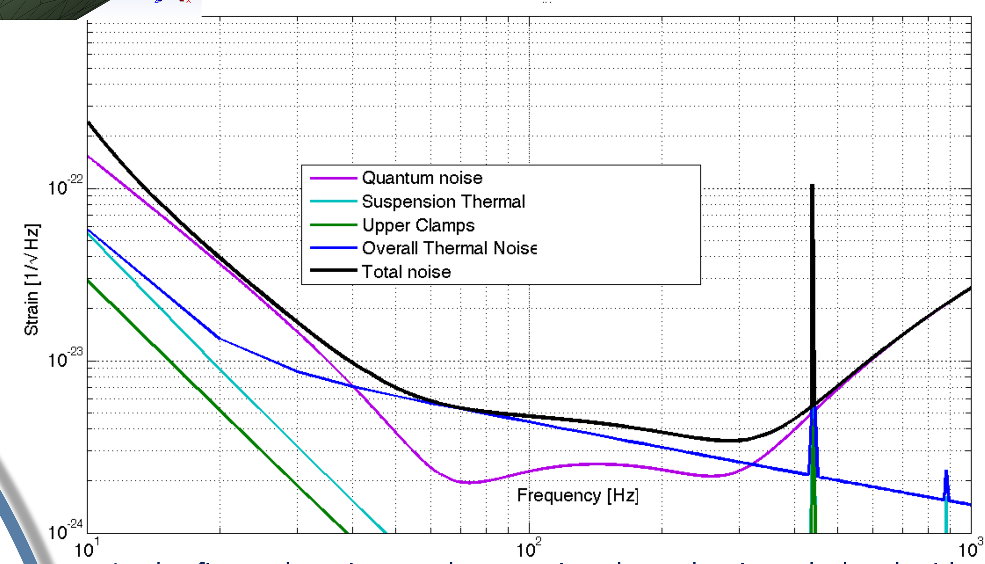

In the figure the mirror and suspension thermal noise calculated with FEM is compared with the Advanced Virgo sensitivity curve (black). In the frequency range of 40-400 Hz the coating thermal noise is the main contributor, while below 40 Hz the radiation pressure dominates (cyan). Above 400 Hz the sensitivity is limited by the shot noise (cyan). The suspension thermal including the clamping systems is negligible (light blue). The clamps losses are negligible with respect to the other terms (green).

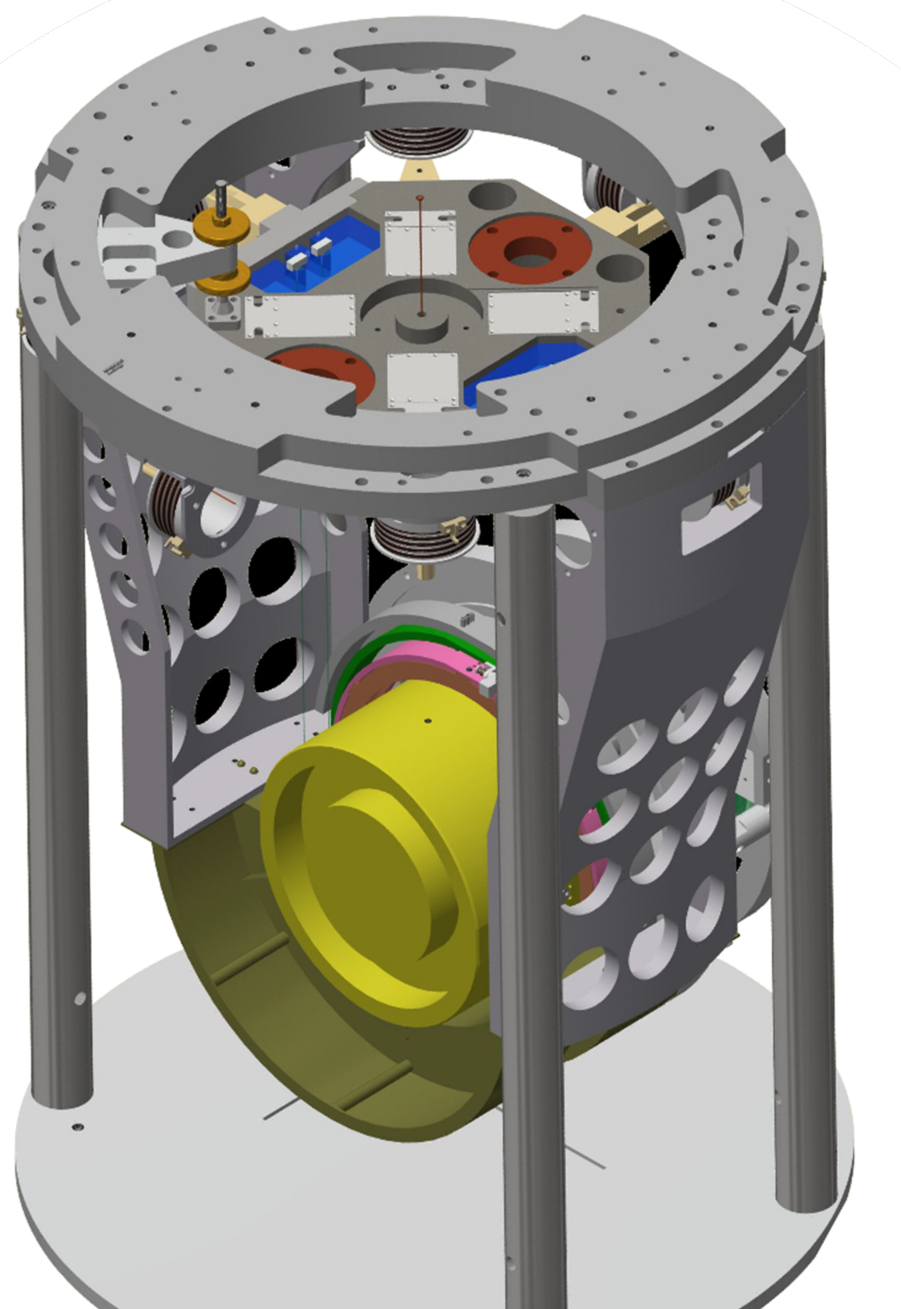

Fibers

CO_2 laser pulling facility

(developed in collaboration with Glasgow people)

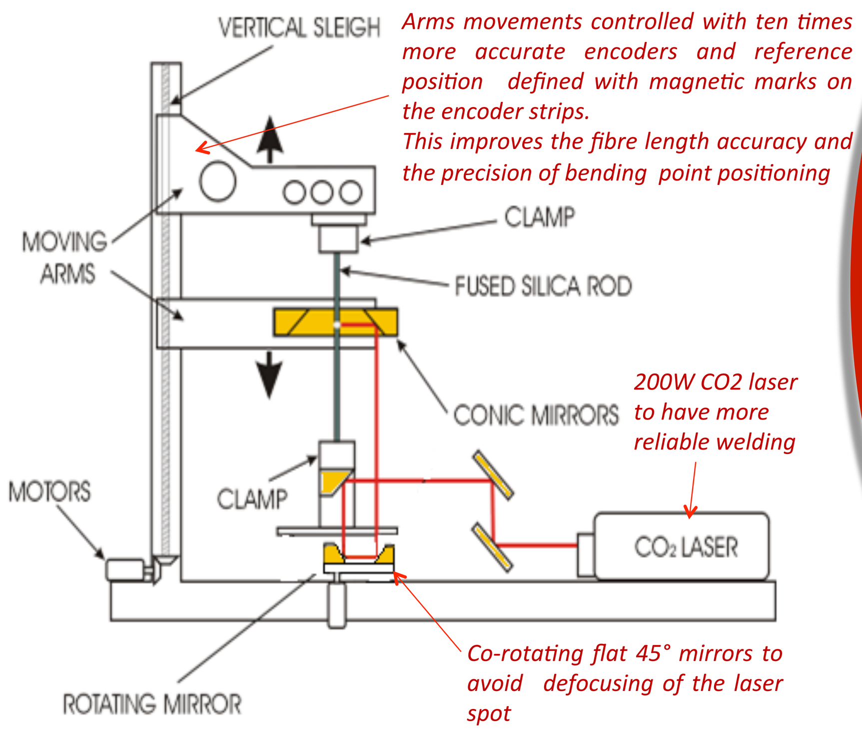

Arms movements controlled with ten times more accurate encoders and reference position defined with magnetic marks on the encoder strips.
This improves the fibre length accuracy and the precision of bending point positioning

200W CO2 laser to have more reliable welding

Co-rotating flat 45° mirrors to avoid defocusing of the laser spot

The Bending Point Machine

Measure of bending points position, violin and bouncing modes frequencies.

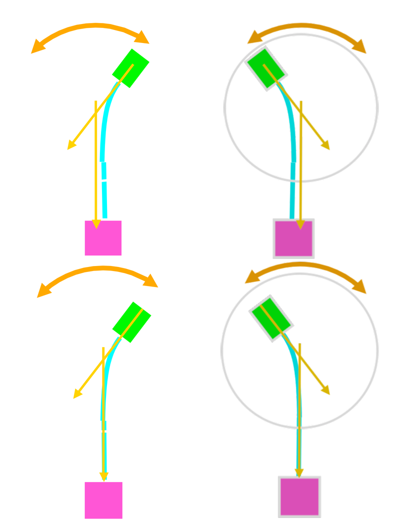

When the horizontal displacement is zero the bending point is on the rotation center

Bending machine measurements

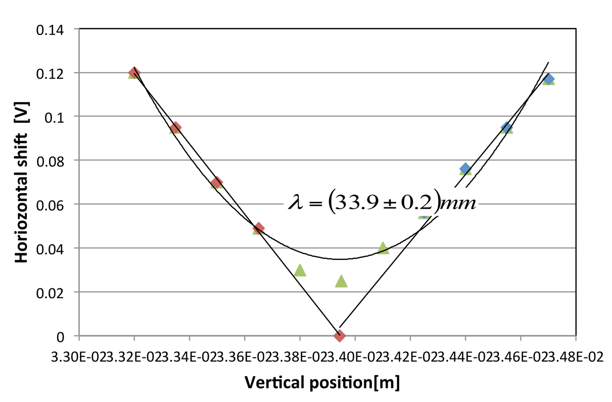

Finite elements model

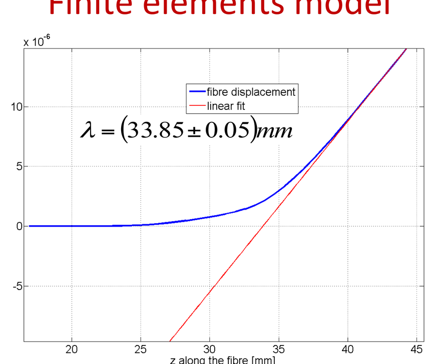

Results comparison between the bending length measurement and a FEM estimation

Fibers Shape

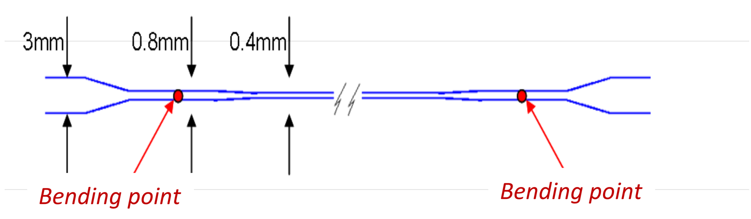

Dumb-bell shaped fibre (aLIGO): fibre diameter 0.4mm to get bouncing < 10Hz and violins > 400Hz with a working load (780MPa) reasonably safe (about the same of Virgo+)

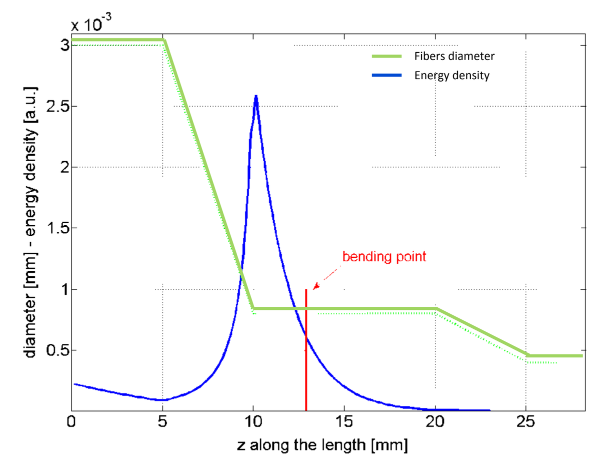

Bending energy stored in 0.8mm region to drop thermo-elastic contribution

Clamps

Upper Clamps

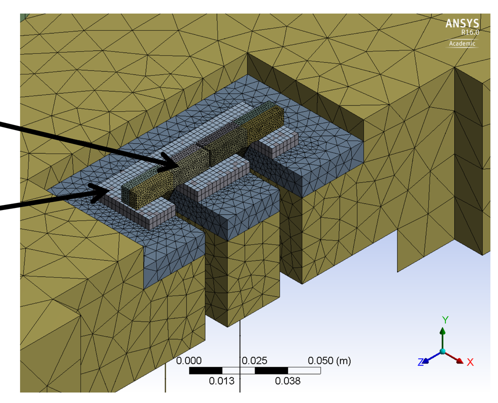

The upper clamp system is formed by a steel plate attached to the marionette where the T-shaped upper tips of the fibers (anchors) are attached with the HCB technique.

Lower Clamps

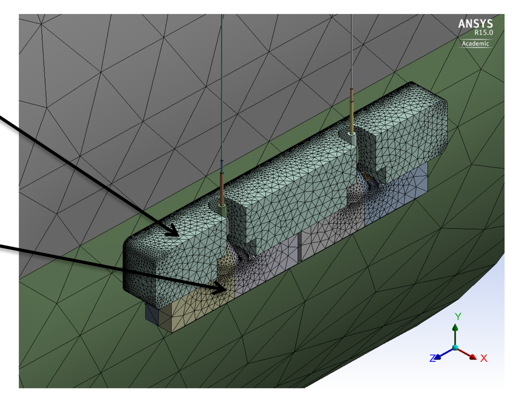

The fused silica ears and anchors provide an appropriate interface to couple the fibers to the mirror lateral sides via the silicate bonds (HCB). The criteria used to make an optimized design of the interface standoff pieces are that the ears must provide a safe interface between the mass and the fibers with a minimum safety factor of 3 in strength. Moreover the thermal noise level for a single test mass resulting from ears and anchors attachment bonds must be lower than the mirror thermal noise level due to its internal and coating losses.

Mirror Box

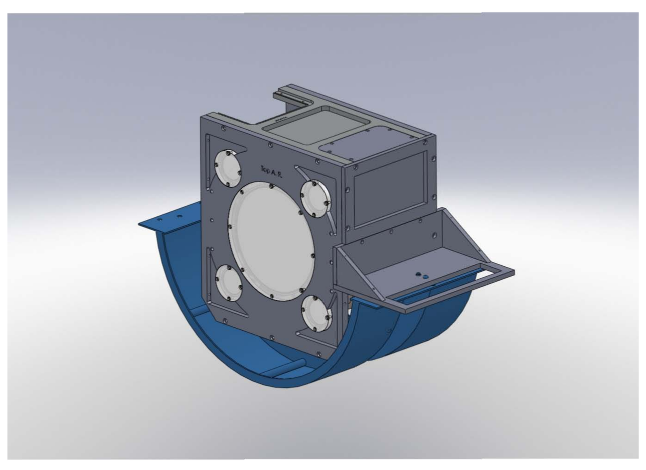

The mirror box allows a safe handling of the mirrors. It is used for positioning the mirrors during the gluing of the ears and the magnets and for positioning the mirror during the assembly in the payload.

References

L. Cunningham et al, Phys. Lett. A, 374 (2010), p.3993; S. Rowan et al, Phys. Lett. A, 347 (2005), p.25; D.H. Gwo, Ultra-precision and reliable bonding method, United States Patent No. US6, 284,085B1, 2001; D.H. Gwo, Hydroxide-catalyzed bonding, United States Patent No. US6, 548,176B1, 2003; M. Lorenzini, VIRGO Collaboration, Class. Quantum Grav., 27 (2010), p. 084007; A. Dari et al, Class. Quantum Grav., 27 (2010), p.045010; G. Cagnoli and P. A. Willems, Phys. Rev. B, 65 (2002), p.174111; P Amico et al, Rev. Sci. Instr., 73 (2002), p.3318; P Amico et al, Class. Quantum Grav., 19 (2002), p.1669; H Vocca, Virgo Collaboration, 12th Marcel Grossmann Meeting on General Relativity, 1 (2012), p.1657; P. Willems, Phys. Lett. A , 300 (2002), p.162; M. Lorenzini et al, Rev. Sci. Instrum., 84 (2013), p.033904

FRONTIER DETECTORS FOR FRONTIER PHYSICS

13th Pisa Meeting on Advanced Detectors
24-30 May 2015 - La Biodola, Isola d'Elba (Italy)